25th International Congress on Modelling and Simulation, Darwin, NT, Australia, 9 to 14 July 2023
mssanz.org.au/modsim2023

Calibration of a physics-based human gastric emptying model

S. Ghosh, P.W. Cleary and S.M. Harrison

CSIRO Data61, Melbourne, Australia
Email: shouryadipta.ghosh@csiro.au

Abstract: The rate of gastric (or stomach) emptying following a meal has important implications for health, including satiety and blood glucose regulation, which relate to obesity and diabetes, and the development of new drug delivery systems. This process is driven by the pressure gradient between the stomach and the duodenum, which is generated by various motility mechanisms such as tonic contraction, antral contraction waves (ACWs), and periodic opening and closing of the pyloric sphincter. Current experimental methods, such as magnetic resonance imaging (MRI), do not accurately measure the emptying rate and all the different aspects of gastric motility simultaneously. Therefore, it remains unclear to what extent the various motility mechanisms independently regulate and affect gastric emptying rate.

This study employs a Smoothed-Particle Hydrodynamics (SPH) based computational model to investigate gastric emptying and uses the results of an MRI based experiment to calibrate the stomach-duodenum pressure gradient along with opening diameter of the pyloric sphincter. The model comprises a realistic 3D surface mesh of the stomach with all major geometric features. Motility mechanisms, such as antral contraction waves (ACWs) and a periodically opening pylorus, are simulated as prescribed deformations of the surface mesh (Figure 1). To simulate the MRI experiment, we integrated as much information about the motility patterns as possible from the MRI analysis. However, sufficient data on two critical parameters was not available: (i) the maximum opening diameter of the pylorus (D_{max}), and (ii) the value of back-pressure (P_D) applied in the proximal duodenum (Figure 1). Hence, these parameters were calibrated to match the experimental emptying rate, which allowed for an investigation into the interplay between these parameters and understanding of their impact on the gastric emptying rate.

The simulation results show that the gastric emptying rate, characterised by emptying half time, is strongly affected by the back pressure, and less affected by the opening diameter of the pylorus. Specifically, the emptying half-time is only moderately affected by D_{max} when P_D is low, while the effect of D_{max} is negligible when P_D is high. The model-predicted emptying half-times showed the closest agreement with the estimation from Marciani et al.'s experiment when P_D was set to 700 Pa and D_{max} to 20 mm. Flow results (shown below) confirm the presence of flow features that are observed by other similar studies, suggesting that current results are valid. These include eddies near the ACWs along the bottom surface of the stomach during pyloric opening and strong upward currents in the same location after pyloric closure. Future extensions of the model will include dynamic solid objects in the gastric content and simulations of longer periods of emptying.

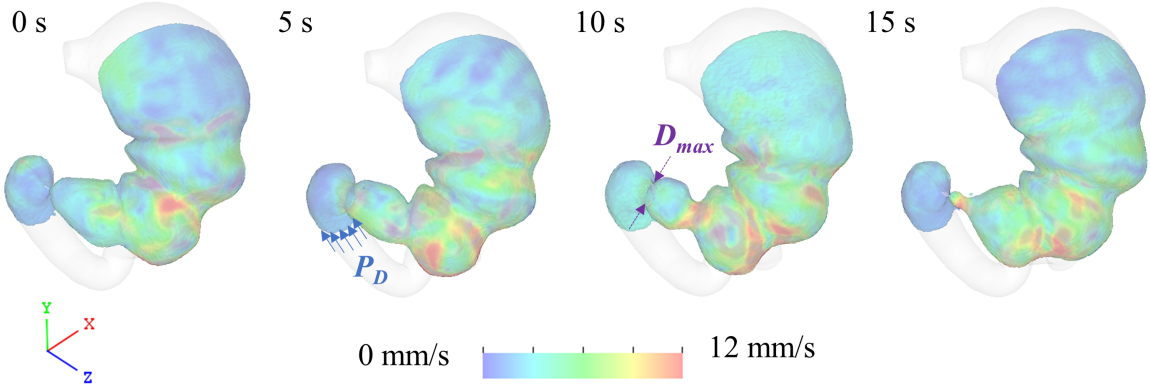

Figure 1. Examples of deformed stomach mesh shapes following application of ACWs. The arrows indicate the backpressure P_D applied at the duodenum and the maximum opening diameter D_{max} of pyloric sphincter. Surface rendering of the digesta is also shown with the colour spectrum representing the velocity of digesta

Keywords: *Stomach, gastric emptying, smoothed-particle hydrodynamics, biomechanics*

1. INTRODUCTION

The human stomach has a critical role in the digestion of food. Its functions include mixing, shearing, grinding, chemical breakdown and transport of the resulting liquid-particulate mixture to the duodenum (which is termed gastric emptying). The rate of gastric emptying affects the overall volume of digesta in the stomach and its resulting distention – which is considered as a key driver of the satiety signal sent to the brain after a meal (Clegg et al., 2013). It further regulates blood glucose concentration (Hlebowicz et al., 2007) which is important for metabolic conditions such as diabetes. It is also a critical factor in the development of novel oral drug delivery systems that are designed for either prolonged retention in the stomach (Tripathi et al., 2019) or rapid release into the duodenum with the rest of the digesta (Meyer et al., 1988).

Gastric emptying is fundamentally driven by two distinct pump mechanisms (Goyal et al., 2019). These are (i) a pressure pump, driven by tonic contraction of the proximal stomach in addition to underlying hydrostatic pressure and (ii) a peristaltic pump, driven by antral contraction waves (ACWs). In addition, (iii) periodic opening and closing of the pyloric sphincter connecting the stomach with duodenum also have a role in regulating the passage of digesta. The motility mechanisms in the stomach have an intrinsic relationship with how the properties of the ingested food and digesta affect the emptying rate.

Previous experimental works show that the gastric emptying rate can undergo large variations based on calorie density (Kwiatek et al., 2009; Marciani et al., 2001b), digesta volume (Kwiatek et al., 2009) and material properties including solid content (Bornhorst et al., 2013) and viscosity (Marciani et al., 2001b, 2001a) of the digesta. For example, when digesta contains little to no calories, the pyloric sphincter remains in a relaxed position with minimum resistance, leading to a fast rate of emptying (Steingoetter et al., 2006). When the caloric density of the digesta is increased, pyloric resistance increases (Heddle et al., 1988) and gastric emptying becomes progressively slower (Schwizer et al., 1996). However, it is not clearly understood how motility patterns in the stomach wall interact with the material properties of digesta to lead to the abovementioned variations in emptying rate.

In contrast to the limitations in experimental methods, in silico models can be a powerful tool for investigating gastric flow because all data is available without measurement effects and individual variables such as pump mechanism properties and digesta properties can be independently controlled. In an early computational study, Pal et al. (2004) used a two-dimensional model of gastric fluid dynamics to study the sensitivity of gastric mixing to different motility parameters such as occlusion and width of ACWs. Subsequently, Ferrua and Singh et al. (2010) developed a 3D model of gastric mixing in a stomach with closed pylorus. In recent years, the Imai (Ebara et al., 2023; Ishida et al., 2019) and Mittal (Kuhar et al., 2022; Seo and Mittal, 2021) groups have separately developed models of gastric fluid dynamics in anatomically realistic 3D stomach geometries, coupled with peristaltic ACWs and periodic pyloric opening. Previously, our group also developed a Smoothed-particle hydrodynamics (SPH) model to investigate emptying of an aqueous digesta (Harrison et al., 2018) through an open pylorus under the effect of peristalsis.

Here we expand the capabilities of the SPH model and calibrate two unknown parameters using data from an experimental study (Marciani et al., 2001a). The improved model includes a periodically closing pylorus that synchronizes with the ACWs, based on recent work by others (Ishida et al., 2019). A parameter study is performed on the pressure difference applied in the outlet boundary condition and the pylorus opening diameter to reproduce measured emptying rates of liquid digesta (Marciani et al., 2001a). This calibration process and analysis is used to investigate how these motility factors affect the gastric emptying rate.

2. METHODS

2.1. Smoothed particle hydrodynamics

SPH is a Lagrangian particle method that offers a mesh-free alternative to solving partial differential equations, as it does not require a fixed grid for discretising the fluid domain unlike Eulerian methods. Its effectiveness in handling complex fluid dynamics problems and large deformations without the need for remeshing has made it a popular choice in various fields of study (Cleary et al., 2021, 2007; Monaghan, 2005). In this method, the volumes of fluids are represented by a moving set of particles, over which the Navier-Stokes equations can be expressed as a set of ordinary differential equations. To model solid boundaries, boundary SPH particles are utilized, whose positions are updated at each time step as a result of wall movements in a deforming surface mesh representing the stomach. Further details about the SPH method employed in the current model can be found in previous studies (Cleary et al., 2021; Harrison et al., 2018).

2.2. Modelling of stomach content and wall motions

In this SPH model the liquid digesta is considered as a Newtonian fluid, represented using SPH particles with average separation (psep) of 1.5 mm. The selection of the psep value of 1.5 mm is based on a separate set of simulations that assessed the convergence of a gastric mixing simulation with varying psep values. The stomach wall in the current simulation is represented by a deforming surface mesh with the same spatial resolution. Figure 2 shows the original surface mesh of the stomach prior to deformation. The mesh is created using Autodesk Maya, a 3D graphics and animation software.

The surface mesh is deformed using an antral contraction wave (ACW) model that involves kinematically prescribed deformations of the stomach mesh (Figure 2). The ACWs originate at the proximal antrum and propagate towards the pylorus with varying amplitude, pulse width, and speed. These parameters were adopted from Ishida et al. (2019), who in turn implemented data from Pal et al. (2004). Pal et al. determined the peristaltic parameters by fitting a cubic spline through selected points in a 2D MRI movie obtained from a single subject after consuming a nutrient-rich meal. Ishida et al. also integrated velocity data from an experiment (Berry et al., 2016) where high-resolution electrophysiological activity data was used to quantify the ACWs in fasted stomachs of patients undergoing hepatobiliary or pancreatic surgery.

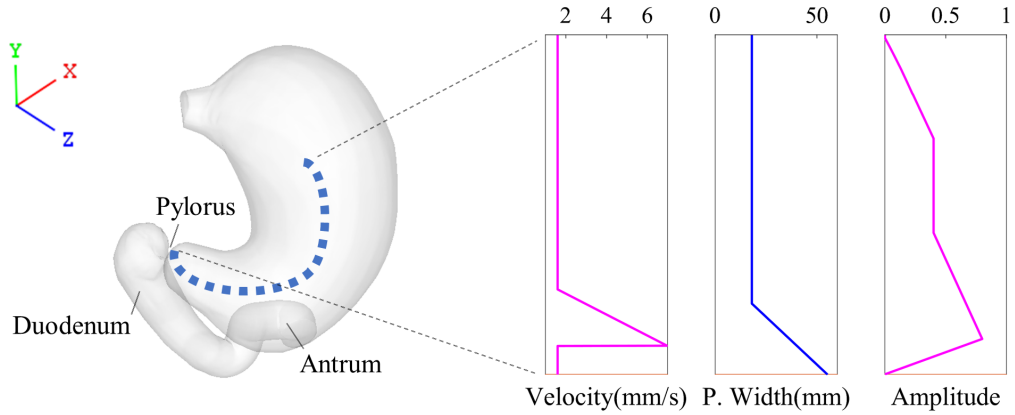

Figure 2. Stomach model geometry. The surface mesh of the stomach is depicted in its resting state. The dotted centreline represents the distance along which ACW waves are applied. An individual wave's velocity, pulse width, and amplitude as a function of distance travelled are illustrated in the insets

The pylorus is prescribed to open in coordination with each ACW (Ishida et al. 2019). However, the three time points when the pylorus is opening, fully opened, and closing are unknown and are calibrated here against the times required for an ACW to reach three specific distances from the pylorus. This location-based coupling between pyloric behaviour and ACW waves is consistent with Indireshkumar et al.'s observation that transpyloric flow is blocked when ACWs reach a "zone of influence" 20-30 mm away from the pylorus (Indireshkumar et al., 2000).

2.3. Model calibration and reproduction of MRI experiment

In Marciani et al.'s experiment, each participant ingested 500 ml of liquid with low calorie content (300 kcal) and a viscosity of 0.06 Pa·s. With each liquid meal, the participants also ingested 15 spherical agar beads with specific fracture strengths and proportionally varying elasticities. MRI images of the subjects were acquired every 15 min, from which the emptying rates and corresponding half-emptying times of the liquid phase of the digesta were calculated. The average emptying curve of the liquid phase was exponential in shape. Marciani et al. also quantified the antral motility parameters from the collected MRI images, such as average values of ACW frequency (~ 3 contractions per min) and speed (~1.56 mm/s). But no data was available about the pyloric dynamics or the pressure applied by tonic contractions and hydrostatic pressure.

To reproduce Marciani et al.'s experiment, 500 ml of liquid with viscosity of 0.06 Pa·s was placed within the model stomach. The density of the meal inside the stomach was assumed to be 1000 Kg/m^3 to account for dilution of the meal by gastric secretions. Digesta flow caused by the ACWs and periodic opening of the pyloric sphincter was simulated for the first two minutes of gastric emptying. Subsequently, an exponential curve was fitted through the initial gastric emptying volume predictions to determine the time required to achieve 50% of emptying. The frequency and speed of the ACWs in these simulations were set to match the values obtained from the experiments.

The two model parameters to be calibrated were (i) the maximum opening diameter of the pylorus (D_{max}) and (ii) value of a backpressure (P_D) which was applied in the proximal duodenum (as shown in Figure 1). In the model, timing and duration of the pylorus opening were assumed to be spatially synchronized with the ACWs, which implied D_{max} is the only aspect of the pyloric opening behaviour which could be varied independent of ACWs. In absence of a model of tonic contraction, P_D could be interpreted as the difference between the actual physiological pressure at the proximal duodenum due to contraction of intestines and the pressure generated in stomach due to tonic contraction. Multiple simulations were run with 3 x 3 = 9 different combinations of these two parameters (D_{max} and P_D) to explore the parameter space for which there is a close fit between model predicted half-emptying times and experimental results.

3. MODEL PREDICTIONS OF GASTRIC FLOW AND EMPTYING

3.1. Flow and mixing within the stomach

Figure 3B shows the flow behaviour of the stomach during a 20 s period between consecutive ACWs. Flow vectors are shown for a 5 mm thick cross-sectional plane through the stomach (whose location is indicated in Figure 3A). The simulation represented in this figure corresponds to a P_D of 700 Pa and D_{max} of 20 mm.

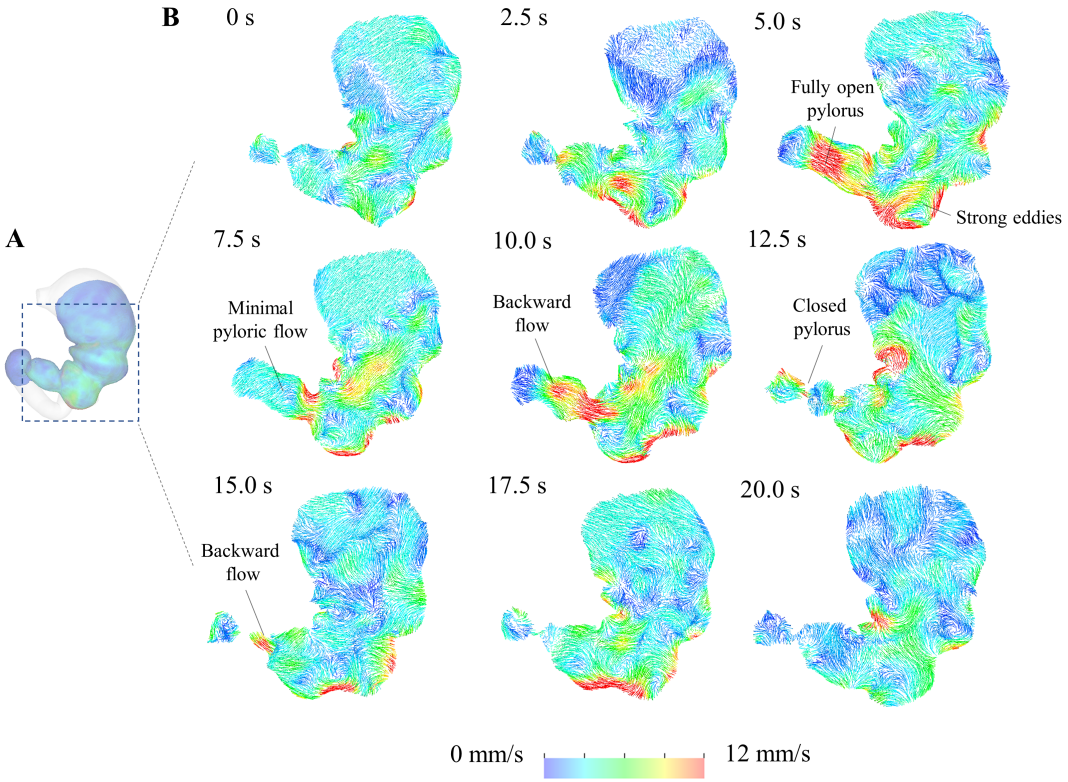

Figure 3. The fluid flow in a cross-sectional plane passing through the centre of the stomach is displayed, demonstrating gradual emptying. (A) The location of a 5 mm thick cross-sectional plane. (B) Speed of the SPH particles within the 5 mm plane is represented by constant-length vectors and is coloured using the spectrum shown at the bottom of the figure

Initially, the pylorus is in a closed position and fluid velocities are small. As the ACWs progress towards the pylorus, the pyloric sphincter begins to relax after 2.5 s and reaches a fully open state by 5 s. At 5 s, there is a noticeable flow through the pylorus from the stomach to the duodenum. High speed eddies can be also noticed near the surface of the stomach, particularly in the proximity of the contracted regions. The intensity and velocity of these eddies are most pronounced in the antral area. After 7.5 s, the pressure between the duodenum and the stomach has equalized due to flow through the open pyloric sphincter. After equalisation, the flow through the sphincter declines and becomes minimal. However, strong eddies persist adjacent to the heavily contracted parts of the stomach wall. Similar eddies have also been observed in a previous modelling study (Pal et al., 2004) and are thought to be critical for mixing but have not been observed in experiments.

At 10 s, the pyloric sphincter begins to contract. The fluid located within the open pyloric channel is dissipated away due to its rapid collapse. This initiates a backward flow from the pylorus towards the antrum, causing a

weakening of the eddies. By 12.5 s, the sphincter is fully closed, leading to a flow of liquid near the closed sphincter towards the duodenum on the duodenal side, while the antral side experiences the complete dissipation of eddies and strong upward liquid motion throughout the stomach. After another 2.5 s, the upward flow in the stomach begins to diminish. But as an ACW approaches the pylorus, its amplitude, pulse width and velocity increase. Subsequently, a strong retrograde flow can be observed in the terminal antral region of the stomach. These predictions are consistent with previous modelling studies that have demonstrated a similar retrograde flow in the terminal antral region (Berry et al., 2016; Ishida et al., 2019). At 15 s, some eddies begin to reappear in the antral region near the stomach wall. However, these eddies weaken considerably again by 20 seconds, resulting in very low flow velocities throughout the stomach.

3.2. Effect of pyloric diameter and pressure difference on gastric emptying rate

Figure 4 displays the range of emptying half-times predicted for different values of D_{max} and P_D. The results indicate that when P_D is smaller the flow rate increases resulting in shorter half-times. There is a nonlinear relationship between emptying half-times and D_{max} which depends on P_D. When P_D is low (600 or 650 Pa) there is a moderately negative correlation between D_{max} and emptying half-times. However, when P_D is higher (at 700 Pa), no clear correlation is observed.

The best agreement between the model-predicted emptying half-times and that estimated from Marciani et al.'s experiment was for P_D = 700 Pa and D_{max} = 20 mm. The results suggest that when the resistance to flow in the duodenum due to P_D is high, the emptying rate might not be sensitive to the maximum extent to which pyloric sphincter is opened. But when the pressure differential across pylorus is lower, the emptying rate becomes sensitive to variation in D_{max}.

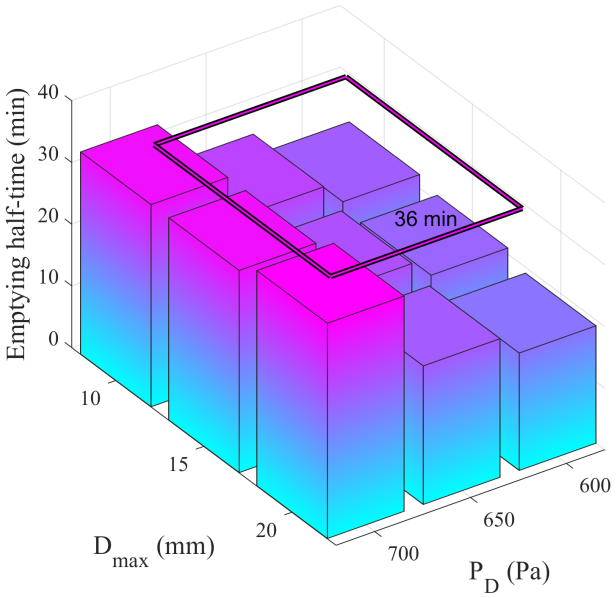

Figure 4. The 3D bar plot displays the emptying half-times for various combinations of D_{max} and P_D, calculated using an exponential decay function based on model predicted initial rates of emptying. The 2D square shaped plane indicates the average emptying half-time from Marciani et al.'s experiments

3.3. Limitations and future work

The current study involved the simulation of emptying of a liquid-only digesta. However, in Marciani et al.'s experiment, participants ingested 15 spherical agar beads with specific fracture strengths along with each liquid meal. In future work, we plan to incorporate the dynamics of the agar beads by representing them as dynamic spherical objects with six degrees of freedom. This will help us to understand the role of the solid phase of a mixed solid-liquid digesta on regulating the emptying rate. Additionally, the current model only captures the first two minutes of the gastric emptying process, but we aim to extend it to substantially longer time periods. The model currently does not yet include a representation of tonic contraction in the fundus, which plays a crucial role in driving gastric emptying over longer periods. This can be potentially addressed by incorporating a description of tonic contraction from existing MRI studies (Banerjee et al., 2020) but further characterisation may be required. With these additional features, the model will have the ability to investigate the role of different phenomena such as ACWs and tonic contraction in the emptying of solid-liquid digesta.

4. CONCLUSION

This study introduces an updated SPH model of gastric emptying of a liquid digesta that integrates ACWs and periodically opening pylorus. It predicts the presence of eddies near the ACWs along the lower surface of the stomach during pyloric opening, which are replaced by strong upward currents after pyloric closure. These flow features predicted by the model are consistent with previous modelling studies, suggesting that simulated gastric emptying rates are viable.

The model is used to predict gastric emptying rates and is calibrated to replicate results from an MRI based experimental dataset. Two parameters representing backpressure at the duodenum and the maximum opening diameter of the pylorus are calibrated to match the experimentally measured emptying half-time. Variation of these parameters show that emptying rate is sensitive to duodenal pressure irrespective of the maximum pyloric diameter. In contrast, the emptying rate is influenced by the maximum pyloric diameter only for lower values of duodenal pressure. Future iterations of the model will include representations of dynamic solid objects and tonic contractions.

REFERENCES

Banerjee, S., Pal, A., Fox, M., 2020. Volume and position change of the stomach during gastric accommodation and emptying: A detailed three-dimensional morphological analysis based on MRI. Neurogastroenterology & Motility 32, e13865.

Berry, R., Miyagawa, T., Paskaranandavadivel, N., Du, P., Angeli, T.R., Trew, M.L., Windsor, J.A., Imai, Y., O'Grady, G., Cheng, L.K., 2016. Functional physiology of the human terminal antrum defined by high-resolution electrical mapping and computational modeling. American Journal of Physiology-Gastrointestinal and Liver Physiology 311, G895–G902.

Bornhorst, G.M., Kostlan, K., Singh, R.P., 2013. Particle size distribution of brown and white rice during gastric digestion measured by image analysis. Journal of food science 78, E1383–E1391.

Cleary, P.W., Harrison, S.M., Sinnott, M.D., Pereira, G.G., Prakash, M., Cohen, R.C., Rudman, M., Stokes, N., 2021. Application of SPH to single and multiphase geophysical, biophysical and industrial fluid flows. International Journal of Computational Fluid Dynamics 35, 22–78.

Cleary, P.W., Prakash, M., Ha, J., Stokes, N., Scott, C., 2007. Smooth particle hydrodynamics: status and future potential. Progress in Computational Fluid Dynamics, an International Journal 7, 70–90.

Clegg, M., Ranawana, V., Shafat, A., Henry, C., 2013. Soups increase satiety through delayed gastric emptying yet increased glycaemic response. European journal of clinical nutrition 67, 8–11.

Ebara, R., Ishida, S., Miyagawa, T., Imai, Y., 2023. Effects of peristaltic amplitude and frequency on gastric emptying and mixing: a simulation study. Journal of the Royal Society Interface 20, 20220780.

Ferrua, M., Singh, R., 2010. Modeling the fluid dynamics in a human stomach to gain insight of food digestion. Journal of food science 75, R151–R162.

Goyal, R.K., Guo, Y., Mashimo, H., 2019. Advances in the physiology of gastric emptying. Neurogastroenterology & Motility 31, e13546.

Harrison, S.M., Cleary, P.W., Sinnott, M.D., 2018. Investigating mixing and emptying for aqueous liquid content from the stomach using a coupled biomechanical-SPH model. Food & function 9, 3202–3219.

Heddle, R., Fone, D., Dent, J., Horowitz, M., 1988. Stimulation of pyloric motility by intraduodenal dextrose in normal subjects. Gut 29, 1349–1357.

Indireshkumar, K., Brasseur, J.G., Faas, H., Hebbard, G.S., Kunz, P., Dent, J., Feinle, C., Li, M., Boesiger, P., Fried, M., 2000. Relative contributions of "pressure pump" and "peristaltic pump" to gastric emptying. American Journal of Physiology-Gastrointestinal and Liver Physiology 278, G604–G616.

Ishida, S., Miyagawa, T., O'Grady, G., Cheng, L.K., Imai, Y., 2019. Quantification of gastric emptying caused by impaired coordination of pyloric closure with antral contraction: a simulation study. Journal of the Royal Society Interface 16, 20190266.

Kuhar, S., Lee, J.H., Seo, J.-H., Pasricha, P.J., Mittal, R., 2022. Effect of Antral Motility on Food Hydrolysis and Gastric Emptying from the Stomach: Insights from Computational Models. arXiv preprint arXiv:2208.06668.

Kwiatek, M.A., Menne, D., Steingoetter, A., Goetze, O., Forras-Kaufman, Z., Kaufman, E., Fruehauf, H., Boesiger, P., Fried, M., Schwizer, W., 2009. Effect of meal volume and calorie load on postprandial gastric function and emptying: studies under physiological conditions by combined fiber-optic pressure measurement and MRI. American Journal of Physiology-Gastrointestinal and Liver Physiology 297, G894–G901.

Marciani, L., Gowland, P.A., Fillery-Travis, A., Manoj, P., Wright, J., Smith, A., Young, P., Moore, R., Spiller, R.C., 2001a. Assessment of antral grinding of a model solid meal with echo-planar imaging. American Journal of Physiology-Gastrointestinal and Liver Physiology 280, G844–G849.

Marciani, L., Gowland, P.A., Spiller, R.C., Manoj, P., Moore, R.J., Young, P., Fillery-Travis, A.J., 2001b. Effect of meal viscosity and nutrients on satiety, intragastric dilution, and emptying assessed by MRI. American Journal of Physiology-Gastrointestinal and Liver Physiology 280, G1227–G1233.

Meyer, J.H., Elashoff, J., Porter-Fink, V., Dressman, J., Amidon, G.L., 1988. Human postprandial gastric emptying of 1–3-millimeter spheres. Gastroenterology 94, 1315–1325.

Monaghan, J., 2005. 76399: Smoothed particle hydrodynamics. vol. 68. Rep Prog Phys 1703–1759.

Pal, A., Indireshkumar, K., Schwizer, W., Abrahamsson, B., Fried, M., Brasseur, J.G., 2004. Gastric flow and mixing studied using computer simulation. Proceedings of the Royal Society of London. Series B: Biological Sciences 271, 2587–2594.

Schwizer, W., Fraser, R., Borovicka, J., Asal, K., Crelier, G., Kunz, P., Boesiger, P., Fried, M., 1996. Measurement of proximal and distal gastric motility with magnetic resonance imaging. American Journal of Physiology-Gastrointestinal and Liver Physiology 271, G217–G222.

Seo, J.H., Mittal, R., 2021. Computational Modeling of Drug Dissolution in the Human Stomach. Frontiers in Physiology 2080.

Steingoetter, A., Fox, M., Treier, R., Weishaupt, D., Marincek, B., Boesiger, P., Fried, M., Schwizer, W., 2006. Effects of posture on the physiology of gastric emptying: a magnetic resonance imaging study. Scandinavian journal of gastroenterology 41, 1155–1164.

Tripathi, J., Thapa, P., Maharjan, R., Jeong, S.H., 2019. Current state and future perspectives on gastroretentive drug delivery systems. Pharmaceutics 11, 193.